

PAPER

View Article Online
View Journal | View IssueCite this: *RSC Adv.*, 2019, 9, 12146

Received 8th March 2019

Accepted 8th April 2019

DOI: 10.1039/c9ra01787a

rsc.li/rsc-advances

Pseudonectrins A–D, heptaketides from an endophytic fungus *Nectria pseudotrichia*†

Peinan Fu,^{ab} Tingnan Zhou,^{ab} Fengxia Ren,^b Shuaiming Zhu,^b Yang Zhang,^{id}*^b Wenying Zhuang^c and Yongsheng Che^{*bd}

Four new heptaketides, pseudonectrins A–D (1–4), and four known compounds (5–8) were isolated from cultures of an endophytic fungus *Nectria pseudotrichia*. Their structures were elucidated primarily by NMR experiments. The absolute configurations of 1–3 and 4 were assigned by electronic circular dichroism calculations and the modified Mosher method, respectively. Compound 1–3 showed moderate cytotoxicity, with IC₅₀ values of 11.6–41.2 μM.

Introduction

Heptaketides are a subgroup of polyketides showing diverse structural features and biological effects. To date, a variety of heptaketides including pyranonaphthoquinones,^{1–3} naphthoquinones,⁴ and other rearranged,⁵ ring-opened,^{6,7} or dimeric⁸ derivatives, have been encountered as fungal secondary metabolites, and showed a broad spectrum of biological activities, such as antibacterial, antifungal, and anti-tumor effects.^{1–4} Natural products incorporating a quinone moiety have been the subject of intensive investigations due to their potent antitumor activity. Notable examples are clinically used drugs anthracyclines and mitomycins,⁹ and vitamin K and its synthetic derivative menadione.^{10–12}

The species of fungal genus *Nectria* are well-known for the production of highly colored naphthoquinone derivatives structurally related to fusarubin and bostrycoidin.^{10,13–18} While *Nectria pseudotrichia*, usually considered as a plant pathogen, has been reported to produce naphthoquinones, isocoumarins, and terpenoids.^{19–21} During our continuous search for new cytotoxic metabolites from the plant endophytic fungi,^{22–29} a strain of *Nectria pseudotrichia*, isolated from the twigs of an identified tree on Tiantangzhai Mountain, Anhui, People's Republic of China, was grown in a solid-substrate fermentation

culture. An ethyl acetate (EtOAc) extract of the culture showed cytotoxic effects towards a small panel of four human tumor cell lines. Fractionation of the extract afforded four new heptaketides, which we named pseudonectrins A–D (1–4; Fig. 1), and four known compounds (5–8; Fig. 1). Details of the isolation, structure elucidation, and cytotoxicity evaluation of these compounds are reported herein.

Results and discussion

Pseudonectrin A (1) was assigned a molecular formula of C₂₀H₂₂O₇ (10 degrees of unsaturation) by HRESIMS. Its UV spectrum showed absorptions at 216, 267, and 415 nm, implying the presence of a pyranonaphthoquinone moiety.³⁰ Its IR absorption bands at 1665 cm^{−1} suggested the presence of quinone carbonyl functions. Analysis of its NMR data (Table 1) revealed the presence of five methyl groups including two *O*-methyls, one oxygenated methylene, three oxymethines, one doubly oxygenated quaternary carbon (δ_C 95.2), eight aromatic carbons with two oxygenated (δ_C 162.2 and 165.1) and two protonated (δ_C 103.9 and 104.2), and two ketone carbons (δ_C 181.7 and 182.9). These data accounted for six of the 10 unsaturation calculated from the molecular formula, which

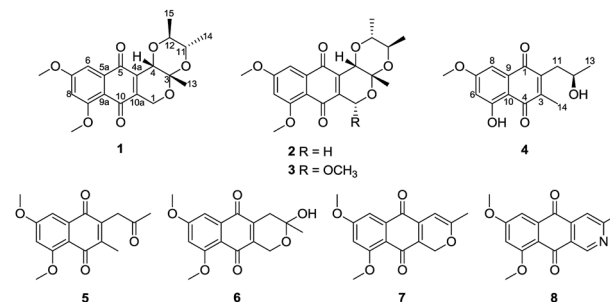


Fig. 1 Structures of compounds 1–8.

^aSchool of Medicine and Life Sciences, Nanjing University of Chinese Medicine, Nanjing 210023, People's Republic of China

^bState Key Laboratory of Toxicology & Medical Countermeasures, Beijing Institute of Pharmacology & Toxicology, Beijing 100850, People's Republic of China. E-mail: cheys@im.ac.cn; zhangyang@bmi.ac.cn

^cState Key Laboratory of Mycology, Institute of Microbiology, Chinese Academy of Sciences, Beijing 100101, People's Republic of China

^dInstitute of Medicinal Biotechnology, Chinese Academy of Medical Sciences & Peking Union Medical College, Beijing 100050, People's Republic of China

† Electronic supplementary information (ESI) available: UV, IR, HRESIMS, NMR spectra of compounds 1–4; ECD calculations of compounds 1–3. See DOI: 10.1039/c9ra01787a

Table 1 NMR data of 1–4

No.	1		2		3		4	
	δ_C^a , type	δ_H^b (J in Hz)	δ_C^a , type	δ_H^b (J in Hz)	δ_C^a , type	δ_H^b (J in Hz)	δ_C^a , type	δ_H^b (J in Hz)
1a	62.3, CH ₂	5.03, d (20.3)	62.5, CH ₂	5.03, d (20.5)	96.2, CH	5.74, s	185.2, qC	
1b		4.67, d (20.3)		4.68, d (20.5)				
2							144.6, qC	
3	95.2, qC		94.9, qC		95.1, qC		145.7, qC	
4	58.7, CH	4.58, s	66.5, CH	4.44, s	66.3, CH	4.42, s	188.6, qC	
4a	136.0, qC		135.8, qC		136.3, qC			
5	182.9, qC		182.7, qC		183.6, qC		164.2, qC	
5a	136.2, qC		136.2, qC		135.8, qC			
6	103.9, CH	7.28, d (2.4)	104.0, CH	7.29, d (2.4)	103.5, CH	7.28, d (2.4)	106.1, CH	6.62, d (2.0)
7	165.1, qC		165.1, qC		164.9, qC		165.9, qC	
8	104.2, CH	6.71, d (2.4)	104.1, CH	6.71, d (2.4)	104.5, CH	6.73, d (2.4)	107.8, CH	7.16, d (2.0)
9	162.2, qC		162.2, qC		162.2, qC		133.6, qC	
9a	114.2, qC		114.3, qC		114.8, qC			
10	181.7, qC		181.8, qC		180.9, qC		109.7, qC	
10a	145.7, qC		145.6, qC		141.8, qC			
11a	66.6, CH	4.54, dq (3.0, 6.7)	70.7, CH	3.94, dq (6.3, 9.0)	70.7, CH	3.90, dq (6.1, 9.0)	36.8, CH ₂	2.81, s
11b								2.80, d (2.2)
12	72.0, CH	3.84, dq (3.0, 6.7)	76.9, CH	3.52, dq (6.3, 9.0)	76.6, CH	3.48, dq (6.1, 9.0)	67.9, CH	4.04, m
13	20.9, CH ₃	1.29, s	20.8, CH ₃	1.27, s	25.2, CH ₃	1.43, s	24.4, CH ₃	1.31, d (6.1)
14	10.6, CH ₃	1.41, d (6.7)	17.3, CH ₃	1.14, d (6.3)	17.3, CH ₃	1.16, d (6.4)	12.9, CH ₃	2.21, s
15	16.8, CH ₃	1.08, d (6.7)	17.2, CH ₃	1.14, d (6.3)	17.2, CH ₃	1.11, d (6.4)		
1-OCH ₃					57.0, CH ₃	3.62, s		
7-OCH ₃	56.6, CH ₃	3.94, s	56.6, CH ₃	3.95, s	56.6, CH ₃	3.95, s	56.1, CH ₃	3.89, s
9-OCH ₃	56.1, CH ₃	3.95, s	56.1, CH ₃	3.95, s	56.1, CH ₃	3.95, s		
OH-5								12.37, s

^a Recorded at 150 MHz. ^b Recorded at 600 MHz.

suggested that **1** was a tetracyclic compound. The ¹H–¹H COSY NMR data showed isolated spin-system of C-11–C-12 (including C-14 and C-15). On the basis of HMBC correlations from H-6 to C-5, C-5a, and C-9a, and from H-8 to C-9a and C-10, a 1,2,3,5-tetrasubstituted phenyl unit fusing at C-5a/C-9a was deduced. While those correlations from H-1a to C-3, C-4a, and C-10a, H-1b to C-4a, and C-10a, and from H-4 to C-4a, and C-10a established a pyran unit fused to the 1,4-naphthoquinone moiety at C-4a/C-10a, completing the pyranonaphthoquinone partial structure in **1**. The 1,4-dioxane moiety was fused to the pyran ring at C-3/C-4 as evidenced by the correlations from H-4 to C-12, and a four-bond W-type correlation observed from H-13 to C-11 in the HMBC spectrum. Other correlations from the two oxygenated methyl protons to C-7 and C-9, respectively, indicated that these two carbons each bear a methoxy group, while those from H₃-13 to C-3 located the C-13 methyl group at C-3. On the basis of these data, the gross structure of **1** was established as shown.

The relative configuration of **1** was proposed by analysis of the ¹H–¹H coupling constants (Table 1) and NOESY correlations (Fig. 2). NOESY correlations of H-1b with H₃-13 and of H-4 with H₃-13 and H₃-15 indicated that these protons are all on the same face of the ring system, whereas those of H-12 with H₃-14 placed the protons on the opposite face. In addition, the small coupling constant observed between H-11 and H-12 (3.0 Hz) suggested their *cis* relationship,³¹ thereby establishing the relative configuration of **1**.

The absolute configuration of **1** was deduced by comparison of the experimental and simulated electronic circular dichroism (ECD) spectra calculated using the time-dependent density functional theory (TDDFT).³² The ECD spectra of the two possible enantiomers **1a** and **1b** (Fig. S25†) were calculated. A random conformational analysis was performed for **1a** and **1b** using the MMFF94 force field followed by reoptimization at the B3LYP/6-311G(d,p) level afforded the lowest energy conformers (Fig. S25†). The overall calculated ECD spectra of **1a** and **1b** were then generated according to Boltzmann weighting of their lowest energy conformers by their relative energies (Fig. 3). The experimental CD spectrum of **1** correlated well to the calculated

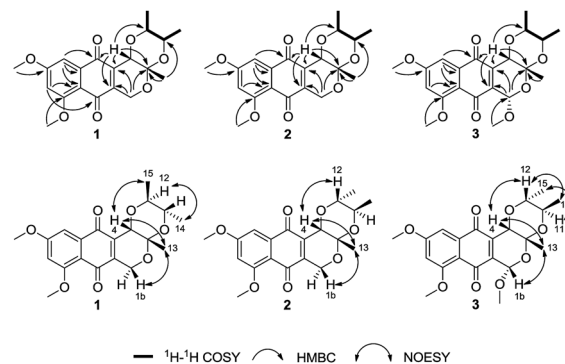


Fig. 2 Key ¹H–¹H COSY, HMBC and NOESY correlations for compounds 1–3.



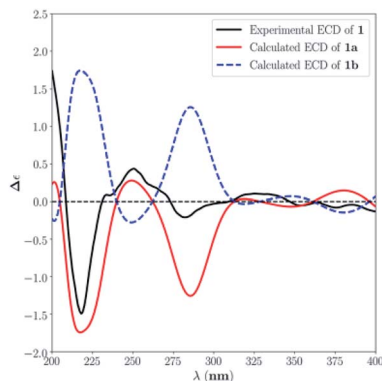


Fig. 3 Experimental CD spectrum of **1** in MeOH and the calculated ECD spectra of **1a** and **1b**.

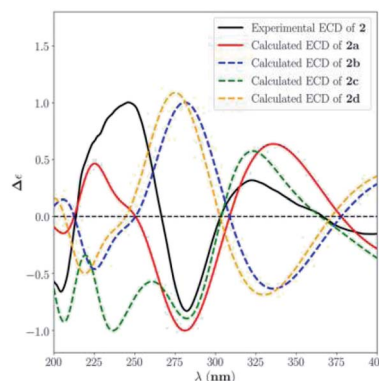


Fig. 4 Experimental CD spectrum of **2** in MeOH and the calculated ECD spectra of **2a–d**.

ECD curve of (3*S*,4*S*,11*S*,12*S*)-**1** (**1a**; Fig. 3), suggesting the 3*S*,4*S*,11*S*,12*S* absolute configuration for **1**.

Pseudonectrin B (**2**) was determined to have the same molecular formula $C_{20}H_{22}O_7$ (10 degrees of unsaturation) as **1** by HRESIMS. Analysis of its 1H and ^{13}C NMR data (Table 1) revealed nearly identical structural features to those found in **1**, except that the chemical shift values for the C-11 and C-12 oxymethines in **2** (δ_H/δ_C 3.94/70.7 and 3.52/76.9) were different from those in **1** (δ_H/δ_C 4.54/66.6 and 3.84/72.0). Interpretation of the NMR data established the same planar structure as **1**, which was supported by relevant 1H - 1H COSY and HMBC data, suggesting that **2** is a stereoisomer of **1**. The relative configuration of **2** was also proposed by analysis of the 1H - 1H coupling constants and NOESY data. NOESY correlations of H-1b with H₃-13 and of H-4 with H₃-13 and H-12 indicated that these protons are on the same face of the molecule. While a large *trans*-diaxial-type coupling constant of 9.0 Hz observed between H-11 and H-12 revealed that these protons were axially oriented.³¹ Therefore, the relative configuration of **2** was proposed.

The absolute configuration of **2** was similarly deduced by comparison of the experimental CD spectrum with the simulated ECD spectra predicted using the TDDFT at the B3LYP/6-311G(d,p) level. The ECD spectra of the four possible isomers **2a–d** (Fig. S26†) were calculated to represent all possible configurations. The experimental CD spectrum of **2** was nearly identical to that calculated for **2a** (Fig. 4), suggesting that **2** has the 3*S*,4*S*,11*R*,12*R* absolute configuration.

The molecular formula of pseudonectrin C (**3**) was determined to be $C_{21}H_{24}O_8$ (10 degrees of unsaturation) based on HRESIMS and the NMR data (Table 1), which is 30 mass units higher than that of **2**. Analysis of the 1H and ^{13}C NMR data for **3** revealed the presence of structural features similar to those found in **2**, except that H-1a (δ 5.03) was replaced by a methoxy unit (δ_H/δ_C 3.62/57.0), and this observation was supported by the HMBC correlations from these newly observed methoxy protons to C-1. Therefore, the gross structure of **3** was established. The relative configuration of **3** was also deduced by analysis of 1H - 1H coupling constants and NOESY data, and by comparison of its 1H NMR data with those of **2**.

The absolute configuration of **3** was assigned by comparison of the experimental CD spectrum with the simulated ECD spectra generated by excited state calculation using TDDFT. The ECD spectra of the two enantiomers **3a** and **3b** (Fig. S27†) were calculated to represent all possible configurations. The MMFF94 conformational search followed by reoptimization at the B3LYP/6-311G(d,p) level afforded the lowest-energy conformers (Fig. S27†). The overall ECD spectra were then generated according to Boltzmann weighting of each conformer. The CD spectrum of **3** correlated well to the calculated curve of **3a** (Fig. 5), suggesting the 1*S*,3*R*,4*S*,11*R*,12*R* absolute configuration.

Pseudonectrin D (**4**) gave a molecular formula of $C_{15}H_{16}O_5$ (eight degrees of unsaturation) by analysis of its HRESIMS. The 1H and ^{13}C NMR data of **4** revealed structural features closely resembled those of the known compound, 2-acetonil-5,7-dimethoxy-3-methyl-1,4-naphthoquinone (**5**).³³ Comparison of their NMR data revealed the presence of an oxymethine (δ_H/δ_C 4.04/67.9) in **4** instead of the ketone functionality in **5** (δ_C 203.9), suggesting that the C-12 carbonyl group in **5** was reduced to a free hydroxy group in **4**. In addition, the methoxy unit (δ_H/δ_C 3.96/56.4) in **5** was replaced by a phenolic hydroxy in **4** (δ_H 12.37), which was supported by the HMBC correlations from the newly observed phenolic proton to C-5, C-6, and C-10.

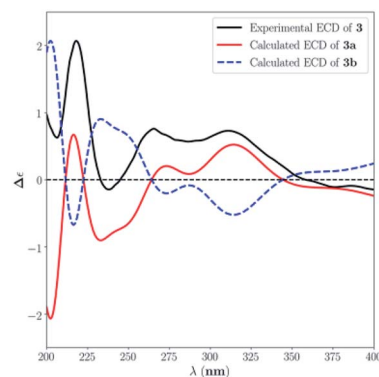


Fig. 5 Experimental CD spectrum of **3** in MeOH and the calculated ECD spectra of **3a** and **3b**.



Therefore, the gross structure of **4** was proposed. The absolute configuration for the C-12 secondary alcohol in **4** was assigned using the modified Mosher method.^{34,35} Treatment of **4** with (*R*)- and (*S*)-MTPA-Cl afforded the (*S*)-(**4a**) and (*R*)-MTPA (**4b**) esters, respectively. The difference in chemical shift values ($\Delta\delta = \delta_S - \delta_R$) for the diastereomeric esters **4a** and **4b** was calculated to assign the 12*R* absolute configuration (Fig. 6).

The other known compounds **6–8** isolated from the crude extract were identified as herbarin (**6**),⁶ dehydroherbarin (**7**),³³ and scorpinone (**8**),³⁶ respectively, by comparison of their NMR and MS data with those reported. The low specific rotation value of **6** $\{[\alpha]_D^{25} +3.7$ (*c* 0.1, MeOH) $\}$ was consistent with the reported one $\{[\alpha]_D^{25} +4.8$ (*c* 0.06, CHCl₃) $\}$,⁶ suggesting that the sample is racemic due to the labile cyclic hemiacetal moiety.⁵

Compounds **1–8** were tested for cytotoxicity against the human tumor cell lines, MCF-7 (breast cancer), HepG2 (hepatocellular carcinoma), SH-SY5Y (glioma), and ACHN (renal cell carcinoma). Compound **1–3**, **6**, and **7** showed moderate cytotoxic effects, with IC₅₀ values of 11.6–45.9 μ M (the positive control cisplatin showed IC₅₀ values of 11.7–18.3 μ M).

Experimental

General experimental procedures

Optical rotations were measured on a Rudolph Research Analytical automatic polarimeter, and UV data were recorded on a Shimadzu Biospec-1601 spectrophotometer. CD spectra were recorded on a JASCO J-815 spectropolarimeter. IR data were recorded using a Nicolet Magna-IR 750 spectrophotometer. ¹H and ¹³C NMR spectra were acquired with Bruker Avance III-600 spectrometers using solvent signals (CDCl₃: δ_H 7.26/ δ_C 77.16) as references. The HSQC and HMBC experiments were optimized for 145.0 and 8.0 Hz, respectively. ESIMS and HRESIMS data were obtained on an Agilent Accurate-Mass-Q-TOF LC/MS G6550 instrument equipped with an ESI source. HPLC analysis and separation were performed using an Agilent 1260 instrument equipped with a variable-wavelength UV detector.

Fungal material

The culture of *N. pseudotrichia* was isolated from twigs of an identified tree on Tiantangzhai Mountain, Anhui, People's Republic of China, in August 2011. The isolate was identified based on morphology and sequence (GenBank accession no. MK305970) analysis of the ITS region of the rDNA. The fungal strain was cultured on slants of potato dextrose agar (PDA) at

25 °C for 10 days. Agar plugs were cut into small pieces (about 0.5 × 0.5 × 0.5 cm³) under aseptic conditions, and 25 pieces were used to inoculate in five 250 mL Erlenmeyer flasks, each containing 50 mL of media (0.4% glucose, 1% malt extract, and 0.4% yeast extract), and the final pH of the media was adjusted to 6.5 and sterilized by autoclave. Five flasks of the inoculated media were incubated at 25 °C on a rotary shaker at 170 rpm for 5 days to prepare the seed culture. Fermentation was carried out in 20 Fernbach flasks (500 mL) each containing 80 g of rice. Distilled H₂O (120 mL) was added to each flask, and the contents were soaked overnight before autoclaving at 15 psi for 30 min. After cooling to room temperature, each flask was inoculated with 5.0 mL of the spore inoculum and incubated at 25 °C for 40 days.

Extraction and isolation

The fermentation material was extracted repeatedly with EtOAc (4 × 4.0 L), and the organic solvent was evaporated to dryness under vacuum to afford 8.6 g of crude extract. The crude extract was fractionated by silica gel vacuum liquid chromatography (VLC) using petroleum ether–EtOAc–MeOH gradient elution. The fraction (45 mg) eluted with 4 : 1 petroleum ether–EtOAc was separated by Sephadex LH-20 column chromatography (CC) eluting with 1 : 1 CH₂Cl₂–MeOH and the resulting subfractions were combined and purified by semipreparative RP HPLC (Agilent Zorbax SB-C₁₈ column; 5 μ m; 9.4 × 250 mm; 78% MeOH in H₂O for 30 min; 2 mL min^{−1}) to afford **7** (2.0 mg, *t*_R 24.1 min). The fraction (110 mg) eluted with 3 : 1 petroleum ether–EtOAc was separated by Sephadex LH-20 CC eluting with 1 : 1 CH₂Cl₂–MeOH, and the resulting subfractions were combined and further purified by RP HPLC to afford **1** (1.0 mg, *t*_R 38.0 min; 42% CH₃CN in H₂O for 50 min; 2 mL min^{−1}), **2** (4.5 mg, *t*_R 42.5 min; the same gradient as in purification of **1**), **3** (1.8 mg, *t*_R 32.5 min; 65% CH₃CN in H₂O for 40 min; 2 mL min^{−1}) and **8** (5.5 mg, *t*_R 22.5 min; the same gradient as in purification of **1**). The fraction (80 mg) eluted with 3 : 2 petroleum ether–EtOAc was separated by Sephadex LH-20 CC eluting with 1 : 1 CH₂Cl₂–MeOH, and the subfractions were combined and purified by RP HPLC to afford **4** (2.8 mg, *t*_R 53.5 min; 40% CH₃CN in H₂O for 60 min; 2 mL min^{−1}) and **5** (4.0 mg, *t*_R 38.0 min; 51% MeOH in H₂O for 45 min; 2 mL min^{−1}). The fraction (50 mg) eluted with 1 : 1 petroleum ether–EtOAc was separated by Sephadex LH-20 CC eluting with 1 : 1 CH₂Cl₂–MeOH, and the subfractions were further purified by RP HPLC to afford **6** (4.0 mg, *t*_R 25.2 min; 57% MeOH in H₂O for 30 min; 2 mL min^{−1}).

Pseudonectrin A (1). Yellow powder, mp 213–214 °C; $[\alpha]_D^{25} +37.0$ (*c* 0.1, MeOH); UV (MeOH) λ_{max} (log ϵ) 216 (4.39), 267 (4.02), 415 (3.39) nm; CD (*c* 5.3 × 10^{−4} M, MeOH) λ_{max} ($\Delta\epsilon$) 218 (−1.50), 250 (+0.44), 282 (−0.21) 325 (+0.10) nm; IR (neat) ν_{max} 2928, 1665, 1592, 1456, 1332, 1276, 1200, 1094, 960, 829, 728 cm^{−1}; ¹H and ¹³C NMR data see Table 1; HMBC data (CDCl₃, 600 MHz) H-1a → C-3, 4, 4a, 10, 10a; H-1b → C-4, 4a, 5, 10a; H-4 → C-3, 4a, 5, 10a, 12, 13; H-6 → C-5, 5a, 7, 8, 9a; H-8 → C-6, 7, 9, 9a, 10; H-11 → C-12, 14; H-12 → C-4; H₃-13 → C-3, 4, 11; H₃-14 → C-11, 12; H₃-15 → C-11, 12; 7-OCH₃ → C-7; 9-OCH₃ → C-9;

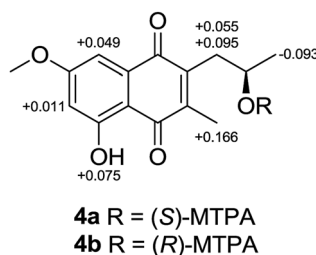


Fig. 6 $\Delta\delta$ values (in ppm) = $\delta_S - \delta_R$ for (*S*)- and (*R*)-MTPA esters of **4**.



NOESY correlations (CDCl₃, 600 MHz) H-1b ↔ H₃-13; H-4 ↔ H₃-13, H₃-15; H-12 ↔ H₃-14; HRESIMS *m/z* 375.1441 [M + H]⁺ (calcd for C₂₀H₂₃O₇, 375.1438).

Pseudonectrin B (2). Yellow powder, mp 219–220 °C; [α]_D²⁵ −96.65 (c 0.1, MeOH); UV (MeOH) λ_{max} (log ε) 217 (4.39), 268 (4.03), 415 (3.44) nm; CD (c 5.3 × 10^{−4} M, MeOH) λ_{max} (Δε) 204 (−0.06), 246 (+1.00), 282 (−0.83) 322 (+0.32) nm; IR (neat) ν_{max} 2916, 1653, 1595, 1457, 1331, 1270, 1216, 1094, 927, 828, 730 cm^{−1}; ¹H and ¹³C NMR data see Table 1; HMBC data (CDCl₃, 600 MHz) H-1a → C-3, 4, 4a, 5, 10a; H-1b → C-4, 4a, 5, 10a; H-4 → C-3, 4a, 5, 10a, 12; H-6 → C-5, 5a, 7, 8, 9a; H-8 → C-6, 7, 9, 9a; H-11 → C-12, 14; H-12 → C-4, 11, 15; H₃-13 → C-3, 4, 11; H₃-14 → C-11, 12; H₃-15 → C-11, 12; 7-OCH₃ → C-7; 9-OCH₃ → C-9; NOESY correlations (CDCl₃, 600 MHz) H-1b ↔ H₃-13; H-4 ↔ H-12, H₃-13; HRESIMS *m/z* 375.1443 [M + H]⁺ (calcd for C₂₀H₂₃O₇, 375.1438).

Pseudonectrin C (3). Yellow powder, mp 220–221 °C; [α]_D²⁵ +74.53 (c 0.1, MeOH); UV (MeOH) λ_{max} (log ε) 218 (4.36), 264 (4.02), 415 (3.43) nm; CD (c 7.2 × 10^{−4} M, MeOH) λ_{max} (Δε) 218 (+2.07), 238 (−0.15), 265 (+0.76) 311 (+0.73) nm; IR (neat) ν_{max} 2919, 1662, 1597, 1467, 1330, 1269, 1197, 1099, 912, 872, 735 cm^{−1}; ¹H and ¹³C NMR data see Table 1; HMBC data (CDCl₃, 600 MHz) H-1 → C-3, 4a, 10a; H-4 → C-3, 4a, 5, 10a, 12, 13; H-6 → C-5, 5a, 7, 8, 9a; H-8 → C-6, 7, 9, 9a; H-11 → C-12, 15; H-12 → C-11, 14; H₃-13 → C-3, 4; H₃-14 → C-3, 11, 12; H₃-15 → C-11, 12; 1-OCH₃ → C-1; 7-OCH₃ → C-7; 9-OCH₃ → C-9; NOESY correlations (CDCl₃, 600 MHz) H-1 ↔ H₃-13; H-4 ↔ H-12, H₃-13; H-11 ↔ H₃-15; H-12 ↔ H₃-14; HRESIMS *m/z* 427.1362 [M + Na]⁺ (calcd for C₂₁H₂₄O₈Na, 427.1363).

Pseudonectrin D (4). Yellow powder, mp 130–131 °C; [α]_D²⁵ +40.0 (c 0.1, MeOH); UV (MeOH) λ_{max} (log ε) 217 (4.14), 268 (3.61), 290 (3.48), 427 (3.11) nm; CD (c 1.8 × 10^{−3} M, MeOH) λ_{max} (Δε) 223 (+0.32), 252 (+0.28), 299 (−0.10), 351 (+0.10), 372 (+0.09) nm; IR (neat) ν_{max} 3384 (br), 2937, 1663, 1631, 1606, 1449, 1338, 1316, 1209, 1031 cm^{−1}; ¹H and ¹³C NMR data see Table 1; HMBC data (CDCl₃, 600 MHz) H-6 → C-5, 8; H-8 → C-1, 6, 7, 10; H-11a → C-1, 2, 12, 13; H-11b → C-1, 2, 12, 13; H-12 → C-2; H₃-13 → C-11, 12; H₃-14 → C-3, 4; 7-OCH₃ → C-7; 5-OH → C-5, 6, 10; HRESIMS *m/z* 277.1073 [M + H]⁺ (calcd for C₁₅H₁₇O₅, 277.1071).

Preparation of (S) and (R)-MTPA esters

A sample of **4** (0.6 mg, 0.002 mmol) was dissolved in 500 μL of anhydrous pyridine. (R)-MTPA-Cl (5.0 μL, 0.026 mmol) was quickly added under nitrogen protection, the mixture was stirred at room temperature for 5 h. The mixture was purified by RP HPLC (Agilent Zorbax SB-C₁₈ column; 5 μm; 9.4 × 250 mm; 95% CH₃CN in H₂O for 15 min; 2 mL min^{−1}) to afford (S)-MTPA ester **4a** (0.3 mg, *t*_R 12.0 min): ¹H NMR (CDCl₃, 600 MHz) δ 12.34 (1H, s, 5-OH), 7.17 (1H, d, *J* = 2.3 Hz, H-8), 6.65 (1H, d, *J* = 2.3 Hz, H-6), 5.30 (1H, m, H-12), 3.91 (3H, s, 7-OCH₃), 2.98 (1H, dd, *J* = 13.4, 4.5 Hz, H-11a), 2.85 (1H, dd, *J* = 13.4, 9.5 Hz H-11b), 2.01 (3H, s, H₃-14), 1.41 (3H, d, *J* = 6.1 Hz, H₃-13).

Similarly, a sample of **4** (0.6 mg, 0.002 mmol), (S)-MTPA-Cl (5.0 μL, 0.026 mmol), and pyridine (500 μL) were processed as described above for **4a**. The mixture was purified by RP HPLC

(Agilent Zorbax SB-C₁₈ column; 5 μm; 9.4 × 250 mm; 95% CH₃CN in H₂O for 15 min; 2 mL min^{−1}) to afford (R)-MTPA ester **4b** (0.3 mg, *t*_R 11.5 min): ¹H NMR (CDCl₃, 600 MHz) δ 12.26 (1H, s, 5-OH), 7.12 (1H, d, *J* = 2.4 Hz, H-8), 6.64 (1H, d, *J* = 2.4 Hz, H-6), 5.27 (1H, m, H-12), 3.92 (3H, s, 7-OCH₃), 2.93 (1H, dd, *J* = 13.4, 3.8 Hz, H-11a), 2.75 (1H, dd, *J* = 13.4, 10.2 Hz, H-11b), 1.84 (3H, s, H₃-14), 1.50 (3H, d, *J* = 6.1 Hz, H₃-13).

Computational details

Conformational analyses for **1–3** were performed *via* the Molecular Operating Environment (MOE) version 2009.10 (Chemical Computing Group, Canada) software package with LowModeMD at the MMFF94 force field. The MMFF94 conformers were further optimized using TDDFT at the B3LYP/6-311G(d,p) basis set level in MeOH with the IEFPCM model. The stationary points have been checked as the true minima of the potential energy surface by verifying that they do not exhibit vibrational imaginary frequencies. The 25 lowest electronic transitions were calculated, and the rotational strengths of each electronic excitation were given using both dipole length and velocity representations. ECD spectra were simulated in Spec-Dis23 (ref. 37) using a Gaussian function with half-bandwidths of 0.30 eV. The overall ECD spectra were then generated according to Boltzmann weighting of each conformer. The systematic errors in the prediction of wavelength and excited-state energies are compensated by employing UV correlation. All quantum computations were performed using the Gaussian 09 package.³⁸

Cytotoxicity assays

The cytotoxic activity of compounds **1–8** were tested using 96 well plates according to a literature MTS method with slight modification.³⁹ Cells were seeded in 96 well plates at a density of 1.0 × 10⁴ cells per well in 100 μL of complete culture medium. After cell attachment overnight, the medium was removed, and each well was treated with 100 μL of medium containing 0.1% DMSO or appropriate concentrations of the test compounds and the positive control cisplatin and incubated with cells at 37 °C for 48 h in a 5% CO₂-containing incubator. Proliferation

Table 2 Cytotoxicity of compound **1–8**

Compound	IC ₅₀ ^a (μM)			
	MCF-7	HepG2	SH-SY5Y	ACHN
1	19.2 ± 4.5	12.5 ± 3.5	17.2 ± 5.1	NA ^b
2	34.2 ± 5.8	29.7 ± 4.7	19.0 ± 2.6	16.8 ± 2.1
3	41.2 ± 4.4	13.3 ± 2.2	NA ^b	11.6 ± 2.5
4	NA ^b	NA ^b	NA ^b	NA ^b
5	29.9 ± 3.4	NA ^b	NA ^b	NA ^b
6	19.2 ± 4.5	45.9 ± 4.0	33.0 ± 4.2	37.0 ± 2.0
7	20.6 ± 4.4	NA ^b	19.3 ± 3.8	12.6 ± 3.3
8	NA ^b	NA ^b	NA ^b	NA ^b
Cisplatin ^c	16.2 ± 2.6	12.8 ± 0.8	18.3 ± 3.6	11.7 ± 2.8

^a IC₅₀ values were averaged from at least three independent experiments. ^b No activity was detected at 50 μM. ^c Positive control.



was assessed by adding 20 μL of MTS (Promega) to each well in the dark, after 90 min of incubation at 37 °C. The optical density was recorded on a microplate reader at 490 nm. Three duplicate wells were used for each concentration, and all the tests were repeated three times.

Conclusions

Pseudonectrins A–C (1–3) are structurally related to a pyranonaphthoquinone metabolite herbarin (6), but differ in possessing an additional 1,4-dioxane ring fused to the dihydropyran moiety at C-3/C-4 of the pyranonaphthoquinone core. Natural products incorporating the 1,4-dioxane unit are relatively rare, most of which were derived from glycosides through the formation of acetal and hemiacetal between aglycone and glycosyl.^{40–44} To our knowledge, pyranonaphthoquinone derivatives with a 1,4-dioxane ring fusing to the dihydropyran moiety have not been reported previously. Pseudonectrin D (4) is structurally related to 2-acetyl-5,7-dimethoxy-3-methyl-1,4-naphthoquinone (5), but differs by having a hydroxy group at C-12 instead of the carbonyl functionality. Compound 5, previously reported as synthetic compound, was isolated as a natural product for the first time. Pyranonaphthoquinone derivatives 1–3, 6, and 7 showed moderate cytotoxic effects, whereas 4 did not show detectable cytotoxicity at 50 μM (Table 2). Biogenetically, 1–8 could be originated from the nonreducing iterative polyketide synthases (NR-PKS),^{5,18} and the hypothetical biosynthetic pathways leading to the generation of these metabolites are illustrated in Scheme S1.†

Conflicts of interest

The authors declare no conflict of interest.

Acknowledgements

P. F., T. Z., S. Z., F. R., and Y. Z. were supported in part by the National Program of Drug Research and Development (2012ZX09301-003); Y. C. was supported by the CAMS Innovation Fund for Medical Sciences (2018-I2M-3-005).

Notes and references

- M. A. Brimble, L. J. Duncalf and M. R. Nairn, *Nat. Prod. Rep.*, 1999, **16**, 267–281.
- J. Sperry, P. Bachu and M. A. Brimble, *Nat. Prod. Rep.*, 2008, **25**, 376–400.
- B. J. Naysmith, P. A. Hume, J. Sperry and M. A. Brimble, *Nat. Prod. Rep.*, 2017, **34**, 25–61.
- A. G. Medentsev and V. K. Akimenko, *Phytochemistry*, 1998, **47**, 935–959.
- W. Geng, X. Wang, T. Kurtán, A. Mándi, H. Tang, B. Schulz, P. Sun and W. Zhang, *J. Nat. Prod.*, 2012, **75**, 1828–1832.
- P. A. Paranagama, E. M. K. Wijeratne, A. M. Burns, M. T. Marron, M. K. Gunatilaka, A. E. Arnold and A. A. L. Gunatilaka, *J. Nat. Prod.*, 2007, **70**, 1700–1705.
- L. Wang, J. Dong, H. Song, K. Shen, L. Wang, R. Sun, C. Wang, Y. Gao, G. Li, L. Li and K. Zhang, *Planta Med.*, 2009, **75**, 1339–1343.
- S. Lösger, O. Schlörke, K. Meindl, R. Herbst-Irmer and A. Zeeck, *Eur. J. Org. Chem.*, 2007, 2191–2196.
- A. M. Heapy, A. V. Patterson, J. B. Smaill, S. M. F. Jamieson, C. P. Guise, J. Sperry, P. A. Hume, K. Rathwell and M. A. Brimble, *Bioorg. Med. Chem.*, 2013, **21**, 7971–7980.
- K. Takemoto, S. Kamisuki, P. T. Chia, I. Kuriyama, Y. Mizushima and F. Sugawara, *J. Nat. Prod.*, 2014, **77**, 1992–1996.
- F. Y. Wu, W. Liao and H. Chang, *Life Sci.*, 1993, **52**, 1797–1804.
- H. Okayasu, M. Ishihara, M. Satoh and H. Sakagami, *Anticancer Res.*, 2001, **21**, 2387–2392.
- D. Parisot, M. Devys, J. Férézou and M. Barbier, *Phytochemistry*, 1983, **22**, 1301–1303.
- D. Parisot, M. Devys and M. Barbier, *Phytochemistry*, 1990, **29**, 3364–3365.
- D. Parisot, M. Devys and M. Barbier, *J. Antibiot.*, 1991, **44**, 103–107.
- D. Parisot, M. Devys and M. Barbier, *J. Antibiot.*, 1992, **45**, 1799–1801.
- J. Kornsakulkarn, K. Dolsophon, N. Boonyuen, T. Boonruangprapa, P. Rachtawee, S. Prabpai, P. Kongsaree and C. Thongpanchang, *Tetrahedron*, 2011, **67**, 7540–7547.
- T. Awakawa, T. Kaji, T. Wakimoto and I. Abe, *Bioorg. Med. Chem. Lett.*, 2012, **22**, 4338–4340.
- N. R. Ariefa, P. Kristiana, H. H. Nurjanto, H. Momma, E. Kwon, T. Ashitani, K. Tawaraya, T. Murayama, T. Koseki, H. Furuno, N. Usukbayar, K. Kimura and Y. Shiono, *Tetrahedron Lett.*, 2017, **58**, 4082–4086.
- N. R. Ariefa, P. Kristiana, T. Aboshi, T. Murayama, K. Tawaraya, T. Koseki, N. Kurisawa, K. Kimura and Y. Shiono, *Fitoterapia*, 2018, **127**, 356–361.
- B. B. Cota, L. G. Tunes, D. N. B. Maia, J. P. Ramos, D. M. Oliveira, M. Kohlhoff, T. M. A. Alves, E. M. Souza-Fagundes, F. F. Campos and C. L. Zani, *Mem. Inst. Oswaldo Cruz*, 2018, **113**, 102–110.
- E. Li, R. Tian, S. Liu, X. Chen, L. Guo and Y. Che, *J. Nat. Prod.*, 2008, **71**, 664–668.
- G. Ding, L. Jiang, L. Guo, X. Chen, H. Zhang and Y. Che, *J. Nat. Prod.*, 2008, **71**, 1861–1865.
- L. Liu, S. Liu, L. Jiang, X. Chen, L. Guo and Y. Che, *Org. Lett.*, 2008, **10**, 1397–1400.
- L. Liu, Y. Li, S. Liu, Z. Zheng, X. Chen, H. Zhang, L. Guo and Y. Che, *Org. Lett.*, 2009, **11**, 2836–2839.
- L. Liu, S. Niu, X. Lu, X. Chen, H. Zhang, L. Guo and Y. Che, *Chem. Commun.*, 2010, **46**, 460–462.
- L. Liu, T. Bruhn, L. Guo, D. C. G. Götz, B. Brun, A. Stich, Y. Che and G. Bringmann, *Chem.–Eur. J.*, 2011, **17**, 2604–2613.
- L. Liu, H. Gao, X. Chen, X. Cai, L. Yang, L. Guo, X. Yao and Y. Che, *Eur. J. Org. Chem.*, 2010, 3302–3306.
- L. Liu, X. Chen, D. Li, Y. Zhang, L. Li, L. Guo, Y. Cao and Y. Che, *J. Nat. Prod.*, 2015, **78**, 746–753.



- 30 M. V. Kadkol, K. S. Gopalkrishnan and N. Narasimhachari, *J. Antibiot.*, 1971, **24**, 245–248.
- 31 J. Trofast and B. Wickberg, *Tetrahedron*, 1977, **33**, 875–879.
- 32 S. Zhu, F. Ren, Z. Guo, J. Liu, X. Liu, G. Liu and Y. Che, *J. Nat. Prod.*, 2019, **82**, 462–468.
- 33 B. Kesteleyn and N. D. Kimpe, *J. Org. Chem.*, 2000, **65**, 640–644.
- 34 J. A. Dale and H. S. Mosher, *J. Am. Chem. Soc.*, 1973, **95**, 512–519.
- 35 I. Ohtani, T. Kusumi, Y. Kashman and H. Kakisawa, *J. Am. Chem. Soc.*, 1991, **113**, 4092–4096.
- 36 A. Miljkovic, P. G. Mantle, D. J. Williams and B. Rassing, *J. Nat. Prod.*, 2001, **64**, 1251–1253.
- 37 T. Bruhn, A. Schaumlöffel, Y. Hemberger and G. Bringmann, *Chirality*, 2013, **25**, 243–249.
- 38 M. J. Frisch, G. W. Trucks, H. B. Schlegel, G. E. Scuseria, M. A. Robb, J. R. Cheeseman, G. Scalmani, V. Barone, B. Mennucci, G. A. Petersson, H. Nakatsuji, M. Caricato, X. Li, H. P. Hratchian, A. F. Izmaylov, J. Bloino, G. Zheng, J. L. Sonnenberg, M. Hada, M. Ehara, K. Toyota, R. Fukuda, J. Hasegawa, M. Ishida, T. Nakajima, Y. Honda, O. Kitao, H. Nakai, T. Vreven, J. A. Montgomery Jr, J. E. Peralta, F. Ogliaro, M. Bearpark, J. J. Heyd, E. Brothers, K. N. Kudin, V. N. Staroverov, R. Kobayashi, J. Normand, K. Raghavachari, A. Rendell, J. C. Burant, S. S. Iyengar, J. Tomasi, M. Cossi, N. Rega, J. M. Millam, M. Klene, J. E. Knox, J. B. Cross, V. Bakken, C. Adamo, J. Jaramillo, R. Gomperts, R. E. Stratmann, O. Yazyev, A. J. Austin, R. Cammi, C. Pomelli, J. W. Ochterski, R. L. Martin, K. Morokuma, V. G. Zakrzewski, G. A. Voth, P. Salvador, J. J. Dannenberg, S. Dapprich, A. D. Daniels, O. Farkas, J. B. Foresman, J. V. Ortiz, J. Cioslowski and D. J. Fox, *Gaussian 09, Rev D.01*, Gaussian, Inc., Wallingford, CT, 2009.
- 39 N. Zhang, Y. Chen, R. Jiang, E. Li, X. Chen, Z. Xi, Y. Guo, X. Liu, Y. Zhou, Y. Che and X. Jiang, *Autophagy*, 2011, **7**, 598–612.
- 40 Y. Fukuyama, M. Ochi, H. Kasai and M. Kodama, *Phytochemistry*, 1993, **32**, 297–301.
- 41 H. El-askary, J. Hölzl, S. Hilal and E. El-kashoury, *Phytochemistry*, 1993, **34**, 1399–1402.
- 42 Y. Tsujino, J. I. J. Ogoche, H. Tazak, T. Fujimori and K. Mori, *Phytochemistry*, 1995, **40**, 753–756.
- 43 T. Lhinhatrakool and S. Sutthivaiyakit, *J. Nat. Prod.*, 2006, **69**, 1249–1251.
- 44 H. Kawagishi, A. Shimada, R. Shirai, K. Okamoto, F. Ojima, H. Sakamoto, Y. Ishiguro and S. Furukawa, *Tetrahedron Lett.*, 1994, **35**, 1569–1572.

